# Tephra in deglacial ocean sediments south of Iceland: Stratigraphy, geochemistry and oceanic reservoir ages

David J.R. Thornalley*, I. Nick McCave & Harry Elderfield

The Godwin Laboratory for Palaeoclimate Research, Department of Earth Sciences, University of Cambridge, Downing Street, Cambridge, CB2 3EQ, UK.

*Present address: School of Earth and Ocean Sciences, Cardiff University, Main Building, Park Place, Cardiff, CF10 3YE, UK.

**ABSTRACT**

Icelandic tephra layers within deglacial ocean sediment cores from south of Iceland have been detected and their timing with respect to the climate shifts of the last deglaciation constrained. Geochemical analysis of the tephra allowed the likely source volcanic systems to be identified. The previously known Saksunarvatn ash and Vedde ash are recognised and described. Several other major tephra layers are examined: a basaltic eruption(s) of Katla at ~8.4 ka; a basaltic eruption of Katla at ~12.6 ka; a rhyolitic eruption of Katla at ~13.6 ka producing tephra similar in appearance and composition to the Vedde ash; a basaltic eruption of Katla at ~14.0 ka; and two basaltic eruptions of Grímsvötn at ~14.6 ka and ~15.0 ka. Abundant rhyolitic ash with a similar appearance and chemistry to the Vedde ash is found throughout the deglacial interval, predating the Vedde ash by up to 3,000 years, supporting previous suggestions that there were pre-Vedde ash eruptions of rhyolite that may have contributed to North Atlantic Ash Zone 1.

This study expands the tephro-stratigraphic framework of the North Atlantic and provides a marine archive in which the timing of tephra layers (useful as isochrons) can be directly compared to major ocean and climate events of the last deglaciation. Furthermore, by correlating tephra layers and abundance changes in the polar foraminifera, *Neogloboquadrina pachyderma* (sinistral), to equivalent tephra events and inferred abrupt cooling/warming in Greenland ice-cores, contemporaneous $^{14}C$ dated planktonic foraminifera have been used to estimate changes in the surface radiocarbon reservoir age south of Iceland. Consistent with previous studies, larger surface reservoir ages are calculated during late Heinrich Stadial 1 and the Younger Dryas (~2000 years and ~800-1900 years respectively).

**INTRODUCTION**

Attempts to understand the past causes of climate change often hinge upon the accurate assessment of the rate and sequence of climate processes, requiring robust and accurate age control. In this regard, tephra layers found within ice-cores, soil profiles and ocean sediment cores (preferably with high sedimentation rates to minimise bioturbation effects), act as important isochrons, facilitating the synchronisation of climate archives separated by hundreds to thousands of kilometres (Lowe, 2001). The development of a tephro-stratigraphic framework therefore represents an important contribution to the assessment of phase relationships between paleoclimate shifts during past abrupt climate change.

Numerous abrupt and often global climate fluctuations occurred during the last deglaciation with changes in North Atlantic ocean circulation being invoked as a likely cause (e.g., Alley and Clark, 1999). Icelandic tephra layers are well established as valuable chrono-stratigraphic markers across the Northeast (NE) Atlantic during this interval (e.g., Kvamme et al., 1989; Lacasse et al., 1996; Haflidason et al., 2000; Rasmussen et al., 2003; Larsen and Eiríksson, 2008), allowing hypotheses regarding the phasing of climate processes to be tested.

Increased volcanic activity of Iceland during the last deglaciation, likely a result of deglacial unloading (Jull and McKenzie, 1996; Maclennan et al., 2002), produced numerous prominent Icelandic tephra layers, including the basaltic Saksunarvatn ash (10.3 ka) and the bimodal Vedde ash (12.1 ka). (The rhyolitic tephra associated with the Vedde ash, widely dispersed across the North Atlantic, is commonly referred to as North Atlantic Ash Zone I (NAAZ-1), although several studies have suggested that there were earlier eruptions producing rhyolitic tephra (Bond et al., 2001; Koren et al., 2008).) In addition to these major eruptions, numerous Icelandic crypto-tephra layers can be identified in soil profiles from Scotland, the Faroe Islands and Scandinavia, including the Dimna Ash (~15.1 ka), Borrobol Tephra (~14.4 ka) and Penifiler tephra (~14.0 ka) (Turney et al., 1997; Davies et al., 2003; Pyne-O'Donnell et al., 2008; Koren et al., 2008).

Detailed analysis of tephra layers found within the NGRIP ice core (Mortensen et al., 2005; Davies et al., 2010) has further advanced the North Atlantic tephro-stratigraphic framework, allowing marine and terrestrial records to be correlated with the well dated, high resolution Greenland ice-cores. Furthermore, by correlating Icelandic tephra layers within marine sediments to similar, well-dated, terrestrial and ice-core deposits, past surface ocean radiocarbon reservoir ages ($R_{surf}$) can be reconstructed, previous studies demonstrating significant variability in $R_{surf}$ throughout the deglaciation and Holocene (Bard et al., 1994; Austin et al., 1995; Eiríksson et al., 2004).

In this study we analyse Icelandic tephra layers within ocean sediment cores taken from the South Iceland Rise, acquired on Charles Darwin cruise 159 for the RAPID programme of NERC (McCave, 2005). We build upon previous studies (e.g. Björck et al., 1992; Lackschewitz et al., 1997; Lacasse et al., 1996; 1998; Haflidason et al., 2000) by placing Icelandic tephra layers within a detailed stratigraphic framework for the last deglaciation. Moreover, the cores used in this study have provided high resolution paleoceanographic evidence for abrupt changes in North Atlantic circulation,

freshwater input, and climate over the last 21 ka (Thornalley et al., 2009; 2010a; 2010b; 2010c), and they therefore constitute an important archive that constrains the timing of Icelandic tephra layers relative to major ocean and climate events. Previous deglacial age models for the cores, based on tephra correlation with NGRIP and changes in the percent abundance of the polar foraminfera species, *Neogloboquadrina pachyderma* (sinistral), allow $^{14}C$ accelerator mass spectrometer (AMS) dates of mono-specific planktonic foraminifera to be used to reconstruct $R_{surf}$.

In this study ages are expressed as kiloyears before 1950 AD (ka), except where otherwise stated. NGRIP ages are based on the GICC05 age scale (b2k) (Rasmussen et al., 2006) and reported here in kiloyears before 1950 AD.

## MATERIALS AND METHODS

Four sediment cores located on the South Iceland Rise (figure1) are examined: RAPiD-10-1P (62º58.53ôN, 17º35.37ôW, 1237 m); RAPiD-12-1K (62º05.43ôN, 17º49.18ôW, 1938 m); RAPiD-15-4P (62º17.58ôN, 17º08.04ôW, 2133 m); RAPiD-17-5P (61º28.90ôN, 19º32.16ôW, 2303 m); abbreviated to 10-1P, 12-1K, 15-4P and 17-5P. The cores lie on the flanks of the Katla ridges and volcanic sediment is largely derived from the proximal Katla and Grímsvötn volcanic systems, found within the Eastern Volcanic Zone of Iceland (Lacasse et al., 1998).

Previously published deglacial age models (Thornalley et al., 2009; 2010a; 2010b) are based on correlation of tephra layers with those in the NGRIP ice core, and by tying changes in the percent abundance of the polar foraminfera species, *Neogloboquadrina pachyderma* (sinistral) (*Nps*), to abrupt climate transitions recorded by the $\delta^{18}O$ of NGRIP ice. $^{14}C$ AMS dates were obtained on mono-specific planktonic foraminfera close to the major tephra layers, avoiding depths at which tephra was likely to be supplied by gravity flows.

The high sedimentation rates of the cores (typically exceeding 20 cm/ka) limits the effects of bioturbation. Comparing modelled distributions with the exponential decrease of tephra grains up-core of a major tephra input suggests effective mixing depths were ~2 cm or less during high sedimentation rate intervals (Thornalley et al., 2010a).

Tephra layers were identified via a range of techniques, including visual identification, physical property data such a colour reflectance and magnetic susceptibility (MS), X-radiographs, and counts of tephra grains taken from splits of the

150-250 μm fraction. Non-volcanic grains were also counted to distinguish between intervals of increased IRD deposition and volcanic eruptions.

Icelandic tephra layers can be attributed to a likely source volcano because many Icelandic volcanic systems have a distinct chemical signature (e.g. Jakobsson, 1979). The major element geochemistry of tephra from selected horizons was therefore determined by electron microprobe analysis using a 5 WD Cameca SX-100 at the Department of Earth Sciences, University of Cambridge, and expressed as major oxide concentrations (weight percent). Techniques were used to reduce Na loss (Na was analysed first, at low current, for a short time interval, using a defocused beam). For major elements an accelerating voltage of 15kV was used, beam current of 4nA, minimum spot size of 10μm and a counting time of 20s. Synthetic and natural mineral standards were used to calibrate and monitor the reliability of the probe; an accuracy of ± 1% is typical.

## RESULTS AND DISCUSSION

The stratigraphic position of major tephra layers and correlation between cores and with the NGRIP ice-core is illustrated in figure 2. Primarily, tephra layers were detected visually, although colour reflectance data also proved useful (for example, sediment lightness shown in figure 3 for core 15-4P). Additionally, abrupt changes in magnetic susceptibility (MS) were associated with the onset of the Saksunarvatn ash (figure 4). Below follows a description of the individual tephra layers. The geochemistry of individual tephra layers is presented in supplementary tables S1 and S2 and illustrated in figures 5-7.

### Tephra layers prior to Heinrich Stadial 1

Identification of tephra layers during the last glacial interval is somewhat hampered by the continued presence of IRD, and detailed tephra work has not yet been conducted on the RAPiD cores prior to Heinrich Stadial 1. However a prominent 1-2 cm basaltic tephra layer occurs in 17-5P at 1103cm at the end of Dansgaard-Oeschger (D-O) event 3 at ~27.3 ka. Radiocarbon dating of planktonic foraminifera (*Nps*) from this depth yielded an age of 23,860 $^{14}$C years (no reservoir correction applied). Several grains have a similar chemistry to the tephra layer St.2-23.5 (dated at 23,960 $^{14}$C years ï no reservoir correction) found in cores south of Iceland on Gardar drift (Haflidason et al., 2000) and it seems probable that Katla was the likely source, although $K_2O$ and $TiO_2$ concentrations are lower than typical (table S1).

A basaltic volcaniclastic gravity flow occurs at 1272 cm (~34.3 ka) in core 17-5P, consisting of ~5-7 cm of cross laminated black silty sand with a sharp base, grading into ~5 cm of bioturbated brown mud. This is overlain by a second flow at 1262 cm that contains ~5-7 cm of laminated black silt and brown mud. Background sedimentation resumes at ~1256 cm. Tephra shards analysed at 1272 cm depth are sourced from Katla and Veidivötn.

**Tephra G2 and G3 (~14.6 and 15.0 ka)**

Increased IRD deposition south of Iceland during Heinrich Stadial 1 makes tephra layer identification difficult, although abundant un-weathered basalt grains were detected at two separate horizons (tephra G2 and G3) within cores 10-1P (176 cm and 207 cm) and 15-4P (512 cm and 518 cm). Tephra G2 can be identified as a decrease in sediment MS in core 10-1P and an increase in MS in the more distal core 15-4P (figure 4). Low sedimentation rates in core 17-5P prevent the two tephra layers being distinguished, although a peak in basaltic tephra was detected at 977 cm. Tephra G2 and G3 consist of highly vesicular, light-medium brown grains similar in appearance to those associated with the Saksunarvatn ash.

Geochemical analyses suggest these tephra are derived from Grímsvötn (table S1, figure 5). Whereas all shards analyzed within tephra G3 have a similar chemistry, characterized by relatively high $TiO_2$ concentrations (~3.3-3.6%), a bimodal range of compositions was associated with tephra G2, with $TiO_2$ concentrations of ~2.4-2.7% and ~3.4-3.7%. It seems probable that volcanic deposits produced during the earlier eruption of tephra G3 were entrained during deposition of tephra G2.

Although basaltic tephra has been detected within NGRIP between 15.7 ka and the onset of the Bølling at 14.6 ka, none of these tephra are likely to have been sourced from Grímsvötn (Mortensen et al., 2005). Elevated $Ca^{2+}$-corrected sulphate concentrations are recorded in NGRIP at 1607m (~14.7 ka) and 1612m (~15.0 ka) which may possibly be related to the eruptions of tephra G2 and G3; yet no shards were detected within NGRIP at these depths (Mortensen et al., 2005).

**Tephra K3 (~14.0 ka)**

Tephra K3 was visible as a 1.5 cm thick basaltic tephra layer at 500 cm depth in core 15-4P, that was also detected as a prominent minima in sediment lightness and a peak in basalt abundance (figure 3). Grains are dark brown to black, vesicular and blocky (similar in appearance to tephra K2 in 10-1P and tephra K1). Geochemical analyses

suggest the source volcano was Katla. Other RAPiD cores did not have sufficient resolution throughout the Bølling Allerød to detect tephra K3.

Tephra K3 occurs at 14.05 ka (based on linear interpolation between the inferred onset and end of the Older Drays as indicated by %*Nps* changes), during the century-long cold interval of the Older Dryas, making it a useful isochron marking the end of the Bølling. A Katla-derived basalt is found during the Older Drays in NGRIP at a depth of 1573.0m (~14.02 ka; Mortensen et al., 2005) and although the chemistry is very similar to that of tephra K3, the NGRIP 1573.0 m tephra contains elevated $Al_2O_3$ (13.04±0.25% versus a mean of 12.26±0.39% for tephra K3). Either these two tephra layers are the same event and the slight difference in their geochemistry is caused by post-depositional alteration in the marine environment (e.g., Thorseth et al., 1992), or the tephra layers were erupted from distinct but closely spaced eruptions (~30 years or less) of Katla.

The NGRIP 1573.0 m Katla tephra has an identical chemistry to the basaltic component of the Penifiler tephra, found in Scottish sediments (Pyne-Oôdonnell et al., 2008); however the Penifiler tephra layer is reported to have occurred after the Older Dryas, during the Allerød, and so may not correlate with tephra K3 or the NGRIP 1573.0 m tephra. The Penifiler tephra is also associated with rhyolitic shards with a similar composition to the rhyolitic Borrobol tephra (Pyne-Oôdonnell et al., 2008). No rhyolite shards within any of the South Iceland Rise RAPiD cores, at any depths analyzed, had a similar composition to the Penifiler and Borrobol rhyolite (figure 7). Combining this with the fact that the rhyolitic shards of the Penifiler and Borrobol are not typical of rhyolite produced by Katla, it seems to be unlikely that Katla was the source volcano for the Penifiler and Borrobol rhyolitic tephra. More probable is that there were coincident eruptions of Katla and a rhyolite producing volcanic centre (speculated by Haflidason et al. (2000) to be Hekla), as suggested by Pyne-Oôdonnell et al. (2008).

**Tephra R1 (~13.6 ka)**

An abundance peak in rhyolite grains occurs in core 15-4P at 486 cm (~13.6 ka). Geochemical analyses suggest a Katla origin, and their appearance (clear, colourless, platy, cuspate shards and bubble-wall forming shards) and geochemistry is simialr to the rhyolitic component of the Vedde ash, also sourced from Katla; although tephra R1 has distinctly higher $Na_2O_3$ (5.09±0.14%). The peak in rhyolite is not accompanied by an increase in any other lithic grains and therefore it seems unlikely to have been caused by

an increase in IRD delivered to the core site. Although a rhyolitic tephra layer has been identified in NGRIP at a depth of 1553.85m (~13.5 ka), itôs geochemistry differs from that of tephra R1, and instead it is possibly sourced from central volcanoes along the North Iceland rift zone (Mortensen et al., 2005).

Tephra R1 (~13.6 ka) occurs close to the onset of a cold interval (as indicated by an increase in %Nps in core 15-4P at ~13.7 ka) and during the middle of freshwater event IV south of Iceland (Thornalley et al., 2010a) recording freshwater rerouting from the Laurentide ice-sheet (figure 9). Tephra R1 may therefore prove a useful isochron.

**Tephra K2 (~12.6 ka)**

In core 10-1P there is a 1 cm bioturbated black tephra layer at 128 cm (12.6 ka), containing abundant dark brown and black, vesicular, blocky grains (>250 μm). Only a limited number of geochemical analyses were conducted on this tephra layer, indicating tephra of mixed origin, but most of which are derived from Katla (table S1, figure 6). Further geochemical analyses of this tephra layer should be conducted; although the timing of this tephra layer suggests it may correlate with the early YD Katla tephra recently found in cores off the Hebridean Margin (Peters et al., 2010).

An increase in basalt grains (fig. 3) and magnetic susceptibility (fig 4) occurs in 15-4P at 472 cm (~12.8 ka; onset of YD), although these tephra grains are typically paler than tephra K2 in 10-1P and the different age strongly suggests this is a different event. Too few geochemical analyses (3 grains) were conducted to confidently assign a volcanic system, but those grains examined derive from Katla. Again, further work is required.

**Vedde ash (~12.1 ka)**

Within core 10-1P, the Vedde ash consists of a sequence of deposits between 64 and 98 cm. A ~1-2 cm basaltic tephra layer (vesicular dark brown basalt grains sourced from Katla) occurs at 98 cm (figure 6). This is overlain by a muddy, unsorted deposit containing large isolated IRD (~1.5 cm), probably produced during a jökulhlaup. The base of the unit contains no foraminifera indicating the material was either delivered straight from Iceland and entrained very little marine material from the shelf, or entrained sand-sized foraminifera were deposited before the mud flow reached site 10-1P. By 80 cm, this muddy unit contains foraminifera in the >150 micron size fraction, which form an assemblage consistent for the Younger Drays (YD) interval, and show no visual signs of reworking. This may indicate normal sedimentation of foraminifera to

the sea-floor; although diluted by terrigenous mud from Iceland, transported by ice-bergs or resuspension off the shelf. A sharp-based, rhyolite-rich, laminated and cross-laminated, sand layer, coloured black by basaltic silt grains, occurs at 74 cm. Rhyolite from this layer is sourced from Katla (table S2) and typical for the Vedde ash (e.g. Haflidason et al., 2000), whereas the basaltic grains are derived from both Katla and Grímsvötn (table S1), the latter presumably being entrained during jökulhlaups and gravity flows. This layer grades into background sedimentation by ~64 cm. A similar but condensed sequence (between 457 and 463cm) occurs within the more distal core 15-4P, whilst in 17-5P, located farthest from Iceland and with low YD sedimentation rates, the Vedde ash is only recognized as a single peak in rhyolite and basalt grains and the sequence of events observed in 10-1P cannot be distinguished.

The Vedde ash is a useful mid-YD isochron, immediately preceding the onset of Heinrich Event 0 (Hillaire-Marcel and deVernal, 2008), an increase in IRD and decrease in deep ocean ventilation south of Iceland (Thornalley et al., 2010b) and a shift in paleoceanographic and climate conditions in the Nordic Seas (Bakke et al., 2009).

**Pre-Vedde ash rhyolitic eruptions**

In addition to tephra R1, rhyolite grains similar in appearance and chemistry (figure 7, table S2) to the Vedde ash are frequently found within the RAPiD cores before the eruption of the Vedde ash. Because many of these increases in rhyolite abundance coincide with increased IRD, confident identification of primary tephra layers cannot be made. However, consistent with previous studies (Bond et al., 2001; Koren et al., 2008) it seems highly probable that there were eruptions of Katla producing Vedde-like rhyolite prior to the eruption of the Vedde ash.

Bond et al. (2001) proposed that a storage-calving mechanism is a viable cause for NAAZ 1 deposition: Vedde-like rhyolite was deposited onto Icelandic glaciers during earlier eruptions and the subsequent increase in ice-berg calving and dispersal during the Younger Dyas led to a peak in rhyolite deposition (NAAZ 1) throughout the North Atlantic. Although it is certainly possible that increased IRD activity contributed to any early YD deposition of Vedde-like in the North Atlantic, it seems highly unlikely that peak rhyolite deposition in the South Iceland Rise RAPiD cores was caused solely by increased IRD, especially given the close proximity of the cores to Katla and the detailed sequence of events associated with the eruption that has been resolved. The storage-calving mechanism may be applicable for more distal sites, where the primary delivery of rhyolite was via ice-rafting and airborne delivery was minor; yet, for sites

proximal to the South Iceland Rise, the synchroneity of the Vedde ash and the onset of a late YD increase in IRD activity (e.g. Thornalley et al., 2010b) was apparently unrelated.

**Saksunarvatn ash (~10.3 ka)**

The Saksunarvatn ash was only identified visually in 17-5P, as a thin (1-2 cm) black silty layer with a sharp base at 862 cm, and was instead identified in the other cores by an increase in abundance of basaltic grains and a decrease in the lightness of the sediment (e.g. figure 3). Tephra grains highly vesicular and light-medium brown in appearance. X-radiographs clearly show the sharp onset of the Saksunarvatn ash in 12-1K at 460 cm depth (figure 4). Consistent with the work of Andrews et al. (2002) from the North Iceland Shelf, the Saksunarvatn ash is associated with a reduction in MS in the cores located proximal to Iceland, 10-1P and 12-1K. In contrast, because the more distal cores 15-4P and 17-5P contain finer sediment and presumably a higher proportion of biogenic sediment with low MS, the deposition of the Saksunarvatn ash is associated with an increase in MS (figure 4).

Previous studies have shown that the Saksunarvatn ash is derived from the Grímsvötn volcano (e.g. Mangerud et al., 1986). Geochemical analyses on grains within 12-1K and 17-5P indicate the same composition as the Saksunarvatn ash (Mangerud et al., 1986) (and hence, derived from Grímsvötn, figure 5). The similar radiocarbon ages obtained for this event in cores 12-1K, 15-4P and 17-5P confirm they are recording the same tephra layer.

The Saksunarvatn ash produces the first major basalt tephra layer in the RAPiD South Iceland Rise cores following the Younger Dryas-Holocene transition. It is therefore probable that the early Holocene tephra layer identified in 10-1P at 38 cm depth (i.e. shortly following the Younger Dryas-Holocene transition at 51 cm depth) correlates to the Saksunarvatn ash. However low Holocene sedimentation rates and 10-1Pôs close proximity to Iceland and numerous volcanic sources has prevented the confident identification of Saksunarvatn ash grains within 10-1P; instead tephra grains with a mixed origin are detected.

**Tephra K1 (~8.4 ka)**

Within core 15-4P, a tephra layer occurs as a 15 cm laminated and cross-laminated bioturbated black sandy mud with a sharp base at 369 cm depth (8.42±0.04 ka), indicative of a basaltic volcaniclastic gravity flow, here termed tephra K1a. A similar

tephra layer, corresponding to a peak in basalt grains (vesicular, blocky, dark brown and black) is also found at 216 cm depth (8.46±0.04 ka) within core 12-1K, termed here tephra K1b. Geochemical analyses indicate Katla as the source volcano (figure 6, table S1) for both these tephra layers, although there are slight differences in composition, with tephra K1a containing higher $Na_2O$ and lower total FeO. Therefore tephra K1a and K1b may have been sourced from separate, but closely spaced eruptions of Katla, which erupted frequently throughout the early Holocene [e.g. *Óladóttir et al.*, 2007]. Several basalt grains with a similar appearance have been found at 640 cm depth within the more distal core 17-5P. Although geochemical analyses have not been conducted on these grains, an approximate age of ~8.1 ka (note ï no radiocarbon dates have been taken close to this depth within 17-5P) hints at a possible correlation with tephra layer K1a or K1b (figure 8).

It is noted that the GISP2 ice-core records high volcanic sulphate emissions (Zielinski et al., 1997) at ~8.4 ka. Also, because eruptions of Katla are sometimes bimodal, it is possible that tephra K1a or K1b coincides with the Suduroy tephra - a rhyolitic tephra layer derived from Katla at ~7.9-8.2 ka, found in soil sections from the Faroe Islands (Wastegård, 2002).

The final drainage of Glacial Lake Agassiz that triggered the ó8.2 kyr cold eventô has been recorded by planktonic foraminifera Mg/Ca-$\delta^{18}O$ salinity reconstructions in core 12-1K at a depth of 184 -212 cm (8.13 ï 8.42 ka) (Thornalley et al., 2009). Tephra K1b may therefore prove a valuable isochron marking the freshwater outburst of Lake Agassiz.

**Tephra G1 (~8.2 ka)**

Tephra G1, centred at 336 cm within 15-4P, is visible as a black 1-2 cm bioturbated layer containing abundant vesicular dark brown basaltic grains in the >150 µm fraction. Tephra typically contain ~2.9-3.2% $TiO_2$ and ~0.4-0.45% $K_2O$ (similar to the Saksunarvatn ash), suggesting Grímsvötn as the source volcano (Figure 5). Tephra G1 was not detected in the other cores located on the East Katla ridge (10-1P and 12-1K), likely because of low sedimentation rates.

**Surface ocean radiocarbon reservoir ages**

Surface ocean reservoir age ($R_{surf}$) estimates are presented in figure 9 and table 1. These have been calculated by taking the difference between the $^{14}C$ age of the contemporaneous atmosphere (using IntCalõ09; Reimer et al., 2009) and that of the

planktonic foraminifera, using the independent age model derived from the stratigraphic correlation of tephra (Saksunarvatn and Vedde) and % *Nps* to the annual layer counted NGRIP ice-core (Thornalley et al., 2010a; 2010b). (Note ï tephra K2 in core 10-1P was not correlated to tephra Tv-1 in NGRIP (1519.1m depth), nor tephra K3 to the NGRIP 1573.0 m tephra as was done in Thornalley et al. (2010a; 2010b) because of their likely different sources and uncertainty in correlation respectively; but even without these ties, the age-models are unchanged, within error.)

Waelbroeck et al. (2001) assumed that by ~9 ka, the North Atlantic $R_{surf}$ was close to 400 years. Using this assumption causes the onset of freshening south of Iceland, associated with the final drainage of Lake Agassiz (recorded by *G. inflata* south of Iceland, freshwater event I, figure 8), to occur at ~8.4 ka. This timing compares well with the terrestrial evidence for this event dated at 8.47 ka (Barber et al., 1999). If tephra K1 can be identified and dated in ice-core or terrestrial deposits, the assumption of a $R_{surf}$ of 400 years can be tested more robustly.

$R_{surf}$ estimates are consistent with previous studies (e.g. Bard et al., 1994; Austin et al., 1995; Waelbroeck et al., 2001; Peck et al., 2006) suggesting larger $R_{surf}$ values at the end of Heinrich Stadial 1 (~15 ka) and during the YD. Previous authors have suggested that the aging of surface waters was caused by the following: a reduction in the northward flow of well-ventilated subtropical surface waters during weakened ocean overturning; sea-ice limiting air-sea exchange; and mixing with $^{14}C$-depleted intermediate and deep waters (e.g., Waelbroeck et al., 2001; Cao et al., 2007). Of particular interest is the $R_{surf}$ age of 1905±132 years in core 10-1P at ~12.6 ka i.e., during the early YD. The core shows no visible signs of reworking at this interval, planktonic assemblages are typical of the YD and benthic isotopes compare well to nearby cores. The onset of the YD is associated with a decrease in ventilation (increased influence of southern sourced water, SSW) south of Iceland and an expansion of sea-ice and polar surface waters (Thornalley et al., 2010b) and the combined effect of these processes may account for the old $R_{surf}$ values, especially given the deep habitat preference of *Nps* (secondary calcite is formed below the thermocline. Mixing with underlying SSW may have been greater on the South Iceland Rise than compared to more open ocean sites because of coastal upwelling and turbulent mixing caused by interaction with seafloor topography.

$R_{surf}$ estimates from the Northwest (NW) Atlantic, based on U/Th-dated coral $^{14}C$, show only a slight aging of surface water, $R_{surf}$ increasing to ~600 years during the Younger Drays (Cao et al., 2007). Cao et al. (2007) also attribute this surface aging to

enhanced mixing with SSW (they suggest Antarctic Intermediate Water). If mixing with $^{14}C$-depleted SSW was a significant factor contributing to surface water aging during the YD, then the observed difference in $R_{surf}$ between the NE Atlantic and NW Atlantic is not surprising, because the eastern basins are more strongly influenced by inflowing SSW in both the modern ocean and during the last glacial maximum (e.g., Beveridge et al., 1995).

$R_{surf}$ values younger than modern are reconstructed for the early Bølling-Allerød warm interval, possibly as a result of enhanced equilibration of subtropical waters during the preceding interval of reduced Atlantic meridional overturning circulation (AMOC) and/or vigorous convection at the beginning of the Bølling-Allerød associated with a rapid resumption and overshoot of the AMOC, as suggested by modelling studies (Knorr and Lohman, 2007; Liu et al., 2009) and evidence for anomalously warm conditions in the Nordic Seas (Muller et al., 2009). An increase in $R_{surf}$ age to 486±138 years during the Older Drays cold interval (~14.0 ka) was presumably caused by enhanced sea-ice cover limiting air-sea exchange and a decrease in deep convection in the North Atlantic, allowing aging of intermediate and deep waters.

## CONCLUSIONS

The stratigraphy and geochemistry of numerous tephra layers within four sediment cores from the South Iceland Rise have been examined during the last deglaciation. Several of these tephra layers correlate with previously reported tephra: the Saksunarvatn ash (~10.3 ka; Grímsvötn source), the Vedde ash (~12.1 ka, Katla source) and possibly an early Younger Dryas tephra (~12.6 ka; sourced from Katla) and a basaltic tephra at ~14.0 ka, sourced from Katla during the Older Dryas. Other prominent tephra include basaltic tephra at ~8.4 ka, sourced from Katla; a rhyolitic tephra at ~13.6 ka from Katla; and two tephra (at ~14.6 ka and ~15.0 ka) preceding the Bølling-Allerød warm interval, sourced from Grímsvötn.

The Vedde ash is shown to comprise several distinct events: an initial basaltic tephra layer sourced from Katla, overlain by a muddy unsorted deposit containing isolated IRD, and finally, sediments containing abundant rhyolite sourced from Katla, and basalt sourced from both Katla and Grímsvötn, the latter likely being entrained during the occurrence of jökulhlaup and gravity flows.

The identification of existing and new Icelandic tephra layers extends the tephro-stratigraphic framework of the North Atlantic; however more importantly, because extensive paleoceanographic work has been conducted on the South Iceland

Rise RAPiD cores, the timing of these tephra layers can be accurately tied to the major ocean and climate events of the last deglaciation.

Reconstructed surface ocean reservoir ages are in good agreement with earlier studies demonstrating aging of surface waters during Heinrich Stadial 1 and the Younger Drays, whilst slightly younger than modern values are reconstructed for the early Bølling-Allerød.

**Acknowledgements**

We thank the crew of CD-159; Angela Huckle for assistance processing the cores; Linda Booth for helping prepare the $^{14}C$ AMS dates, Keith Grey, Chris Haywood and Chiara Petrone for assistance with electron microprobe sample preparation and analyses. John Maclennan and Sarah Collins are thanked for useful discussions and advice. The editor and two anonymous reviewers are thanked for their time and comments. AMS $^{14}C$ dates were run by the NERC radiocarbon laboratory, East Kilbride, Scotland, U.K. Funding was provided by NERC RAPID grant NER/T/S/2002/00436.

## REFERENCES

Alley, R. B., and Clark, P. U. (1999). The Deglaciation of the Northern Hemisphere: A Global Perspective. *Annu. Rev. Earth Planet Sci* **27,** 149-182.

Andrews, J. T., Geirsdottir, A., Hardardottir, J., Principato, S., Grönvold, K., Kristjansdottir, G. B., Helgadottir, G., Drexler, J., and Sveinbjörnsdóttir, A. (2002). Distribution, sediment magnetism and geochemistry of the Saksunarvatn (10,180 +/- 60 cal. yr BP) tephra in marine, lake, and terrestrial sediments, northwest Iceland. *Journal of Quaternary Science* **17,** 731-745.

Austin, W. E. N., Bard, E., Hunt, J. B., Kroon, D., and Peacock, J. D. (1995). The 14C of the Icelandic Vedde ash: Implications for Younger Dryas marine reservoir age corrections. *Radiocarbon* **37,** 53-63.

Bakke, J., Lie, O., Heegaard, E., Dokken, T., Haug, G. H., Birks, H. H., Dulski, P., and Nilsen, T. (2009). Rapid oceanic and atmospheric changes during the Younger Dryas cold period. *Nature Geoscience* **2,** 202-205.

Barber, D. C., Dyke, A., Hillaire-Marcel, C., Jennings, A. E., Andrews, J. T., Kerwin, M. W., Bilodeau, G., McNeely, R., Southon, J., Moorehead, M. D., and Gagnon, J.-M. (1999). Forcing of the cold event of 8200 years ago by catastrophic drainage of Laurentide lakes. *Nature* **400,** 344-348.

Bard, E., Arnold, M., Mangerud, J., Paterne, M., Labeyrie, L., Duprat, J., Melieres, M.-A., Sønstegaard, E., and Duplessy, J.-C. (1994). The North Atlantic atmosphere-sea surface 14C gradient during the Younger Dryas climatic event. *Earth and*

466 *Planetary Science Letters* **126,** 275-287.
467 Beveridge, N. A. S., Elderfield, H., and Shackleton, N. J. (1995). Deep thermohaline
468 circulation in the low-latitude Atlantic during the last glacial. *Paleoceanography*
469 **10,** 643-660.
470 Björck, S., Ingolfsson, O., Haflidason, H., Hallsdottir, M., and Anderson, N. J. (1992).
471 Lake Torfadalsvatn: A high resolution record of the North Atlantic ash zone I
472 and the last glacial-interglacial environmental changes in Iceland. *Boreas* **21,** 15
473 - 22.
474 Bond, G. C., Mandeville, C., and Hoffmann, S. (2001). Were rhyolitic glasses in the
475 Vedde ash and in the North Atlantic's Ash Zone 1 produced by the same
476 volcanic eruption? *Quaternary Science Reviews* **20,** 1189-1199.
477 Cao, L., Fairbanks, R. G., Mortlock, R. A., and Risk, M. J. (2007). Radiocarbon
478 reservoir age of high latitude North Atlantic surface water during the last
479 deglacial. *Quaternary Science Reviews* **26,** 732-742.
480 Davies, S. M., Wastegård, S., and Wohlfarth, B. (2003). Extending the limits of the
481 Borrobol Tephra to Scandinavia and detection of new early Holocene tephras.
482 *Quaternary Research* **59,** 345-352.
483 Davies, S. M., Wastegård, S., Abbott, P. M., Barbante, C., Bigler, M., Johnsen, S. J.,
484 Rasmussen, T. L., Steffensen, J. P., Svensson, A. (2010). Tracing volcanic
485 events in the NGRIP ice-core and synchronising North Atlantic marine records
486 during the last glacial period. *Earth Planet. Sci. Lett.*,
487 doi:10.1016/j.epsl.2010.03.004
488 Eiriksson, J., Larsen, G., Knudsen, K. L., Heinemeier, J., and Simonarson, L. A. (2004).
489 Marine reservoir age variability and water mass distribution in the Iceland Sea.
490 *Quaternary Science Reviews* **23,** 2247-2268.
491 Haflidason, H., Eiriksson, J., and van Kreveld, S. (2000). The tephrochronology of
492 Iceland and the North Altantic region during the middle and late Quaternary: a
493 review. *Journal of Quaternary Science* **15,** 3-22.
494 Hillaire-Marcel, C., and de Vernal, A. (2008). Stable isotope clue to episodic sea ice
495 formation in the glacial North Atlantic. *Earth and Planetary Science Letters*
496 **268,** 143-150.
497 Jakobsson, S. (1979). Petrology of Recent basalts of the Eastern Volcanic Zone,
498 Iceland. *Acta Naturalia Islandica* **26,** 1-103.
499 Jull, M. and McKenzie, D. (1996). The effect of deglaciation on mantle melting beneath
500 Iceland. *Journal of Geophysical Research-Solid Earth* **101**(B10), 21815-21828.

501 Knorr, G., and Lohmann, G. (2007). Rapid transitions in the Atlantic thermohaline
502 circulation triggered by global warming and meltwater during the last
503 deglaciation. *Geochemistry Geophysics Geosystems* **8**, doi:
504 10.1029/2007gc001604.
505 Koren, J. H., Svendsen, J. I., Mangerud, J., and Furnes, H. (2008). The Dimna Ash - a
506 12.8 14C ka-old volcanic ash in Western Norway. *Quaternary Science Reviews*
507 **27,** 85-94.
508 Kvamme, T., Mangerud, J., Furnes, H., and Ruddiman, W. F. (1989). Geochemistry of
509 Pleistocene ash zones in cores from the North Atlantic. *Norsk Geologisk*
510 *Tidskrift* **69,** 251-272.
511 Lacasse, C., Carey, S., and Sigurdsson, H. (1998). Volcanogenic sedimentation in the
512 Iceland Basin: influence of subaerial and subglacial eruptions. *Journal of*
513 *Volcanology and Geothermal Research* **83,** 47-73.
514 Lacasse, C., Sigurdsson, H., Carey, S., Paterne, M., and Guichard, F. (1996). North
515 Atlantic deep-sea sedimentation of Late Quaternary tephra from the Iceland
516 hotspot. *Marine Geology* **129,** 207-235.
517 Lackschewitz, K. S., and Wallrabe-Adams, H.-J. (1997). Composition and origin of
518 volcanic ash zones in Late Quaternary sediments from the Reykjanes Ridge:
519 evidence for ash fallout and ice-rafting. *Marine Geology* **136,** 209-224.
520 Larsen, G., and Eiriksson, J. (2008). Holocene tephra archives and tephrochronology in
521 Iceland - a brief overview. *Jökull* **58,** 229-250.
522 Liu, Z., Otto-Bliesner, B. L., He, F., Brady, E. C., Tomas, R., Clark, P. U., Carlson, A.
523 E., Lynch-Stieglitz, J., Curry, W., Brook, E., Erickson, D., Jacob, R., Kutzbach,
524 J., and Cheng, J. (2009). Transient Simulation of Last Deglaciation with a New
525 Mechanism for Bølling-Allerød Warming. *Science* **325,** 310-314.
526 Lowe, J. J. (2001). Abrupt climatic changes in Europe during the last glacial interglacial
527 transition: the potential for testing hypotheses on the synchroneity of climatic
528 events using tephrochronology. *Global and Planetary Change* **30,** 73-84.
529 Maclennan, J., Jull, M., McKenzie, D., Slater, L., and Grönvold, K. (2002). The link
530 between volcanism and deglaciation in Iceland. *Geochem., Geophys., Geosyst.*
531 **3,** 10.1029/2001GC000282.
532 Mangerud, J., Furnes, H., and Johansen, J. (1986). A 9000-Year-Old Ash Bed on the
533 Faroe Islands. *Quaternary Research* **26,** 262-265.
534 McCave, I. N. (2005). Cruise Report for R.R.S Charles Darwin Cruise CD159, pp. 1-47.
535 Department of Earth Sciences, University of Cambridge.

536 Mortensen, A. K., Bigler, M., Grönvold, K., Steffensen, J. P., and Johnsen, S. J. (2005).
537 Volcanic ash layers from the Last Glacial Termination in the NGRIP ice core.
538 *Journal of Quaternary Science* **20,** 209-219.
539 Muller, J., Masse, G., Stein, R., and Belt, S. T. (2009). Variability of sea-ice conditions
540 in the Fram Strait over the past 30,000 years. *Nature Geoscience* **2,** 772-776.
541 NGRIP members (2004). High-resolution record of Northern Hemisphere climate
542 extending into the last interglacial period. *Nature* **431,** 147-151.
543 Oladottir, B. A., Sigmarsson, O., Larsen, G., and Thordarson, T. (2007). Katla volcano,
544 Iceland: magma composition, dynamics and eruption frequency as recorded by
545 Holocene tephra layers. *Bulletin of Volcanology* **70,** 475-493.
546 Peck, V. L., Hall, I. R., Zahn, R., Elderfield, H., Grousset, F., Hemming, S. R., and
547 Scourse, J. D. (2006). High resolution evidence for linkages between NW
548 European ice sheet instability and Atlantic Meridional Overturning Circulation.
549 *Earth and Planetary Science Letters* **243,** 476-488.
550 Peters, C., Austin, W. E. N., Walden, J., and Hibbert, F. D. (2010). Magnetic
551 characterisation and correlation of a Younger Dryas tephra in North Atlantic
552 marine sediments. *J. Quaternary Sci.* **25,** 339-347.
553 Pyne-O'Donnell, S. D. F., Blockley, S. P. E., Turney, C. S. M., and Lowe, J. J. (2008).
554 Distal volcanic ash layers in the Lateglacial Interstadial (GI-1): problems of
555 stratigraphic discrimination. *Quaternary Science Reviews* **27,** 72-84.
556 Rasmussen, S. O., Andersen, K. K., Svensson, A. M., Steffensen, J. P., Vinther, B. M.,
557 Clausen, H. B., Siggaard-Andersen, M. L., Johnsen, S. J., Larsen, B. M., Dahl-
558 Jensen, D., Bigler, M., Rothlisberger, R., Fischer, H., Goto-Azuma, K.,
559 Hansson, M. E., and Ruth, U. (2006). A new Greenland ice core chronology for
560 the last glacial termination. *Journal of Geophysical Research* **111,** 16.
561 Rasmussen, T. L., Wastegård, S., Kuijpers, E., van Weering, T. C. E., Heinemeier, J.,
562 and Thomsen, E. (2003). Stratigraphy and distribution of tephra layers in marine
563 sediment cores from the Faeroe Islands, North Atlantic. *Marine Geology* **199,**
564 263-277.
565 Reimer, P. J., Baillie, M. G. L., Bard, E., Bayliss, A., Beck, J. W., Blackwell, P. G.,
566 Ramsey, C. B., Buck, C. E., Burr, G. S., Edwards, R. L., Friedrich, M., Grootes,
567 P. M., Guilderson, T. P., Hajdas, I., Heaton, T. J., Hogg, A. G., Hughen, K. A.,
568 Kaiser, K. F., Kromer, B., McCormac, F. G., Manning, S. W., Reimer, R. W.,
569 Richards, D. A., Southon, J. R., Talamo, S., Turney, C. S. M., van der Plicht, J.,

and Weyhenmeyer, C. E. (2009). INTCAL09 and MARINE09 radiocarbon age calibration curves, 0-50,000 years cal. BP. *Radiocarbon* **51,** 1111-1150.

Thornalley, D. J. R., Elderfield, H., and McCave, I. N. (2009). Holocene oscillations in temperature and salinity of the surface subpolar North Atlantic. *Nature* **457,** 711-714.

Thornalley, D. J. R., Elderfield, H., and McCave, I. N. (2010a). Intermediate and deep water paleoceanography of the northern North Atlantic over the past 21,000 years. *Paleoceanography* **25,** PA1211, doi:10.1029/2009PA001833.

Thornalley, D. J. R., McCave, I. N., and Elderfield, H. (2010b). Freshwater input and abrupt deglacial climate change in the North Atlantic. *Paleoceanography* **25,** PA1201, doi:10.1029/2009PA001772.

Thornalley, D. J. R., Elderfield, H., and McCave, I. N. (2010c). Reconstructing North Atlantic deglacial surface hydrography and its link to the Atlantic overturning circulation. *Global and Planetary Change,* doi:10.1016/j.gloplacha.2010.06.003.

Thorseth, I. H., Furnes, H., Heldal, M.. (1992). The importance of microbiological activity in the alteration of natural basaltic glass. *Geochimica et Cosmochimica Acta* **56,** 845ï 850.

Turney, C. S. M., Harkness, D. D., and Lowe, J. J. (1997). The use of microtephra horizons to correlate Late-glacial lake sediment successions in Scotland. *Journal of Quaternary Science* **12,** 525-531.

Waelbroeck, C., Duplessy, J. C., Michel, E., Labeyrie, L., Paillard, D., and Duprat, J. (2001). The timing of the last deglaciation in North Atlantic climate records. *Nature* **412,** 724-727.

Wastegård, S. (2002). Early to middle Holocene silicic tephra horizons from the Katla volcanic system, Iceland: new results from the Faroe Islands. *Journal of Quaternary Science* **17,** 723-730.

Zielinski, G. A., Mayewski, P. A., Meeker, L. D., Grönvold, K., Germani, M. S., Whitlow, S., Twickler, M. S., and Taylor, K. (1997). Volcanic aerosol records and tephrochronology of the Summit, Greenland, ice cores. *Journal of Geophysical Research-Oceans* **102,** 26625-26640.

601 **Table 1.** Accelerator mass spectrometer $^{14}C$ dates and surface ocean reservoir ages.
602 Surface ocean reservoir ages were obtained by calculating the difference between the
603 measured planktonic foraminifer $^{14}C$ age and the contemporaneous atmospheric $^{14}C$ age,
604 derived from IntCal ô09 (Reimer et al., 2009) using the actual calendar age determined
605 from the independent age model (%*Nps*/tephra tied to NGRIP).

| Lab. code | | Core | Sample depth cm | Species | $^{14}C$ age BP 1950 | Stratigraphic age BP 1950 | IntCalô09 $^{14}C$ age ă | Reservoir age $^{14}C$ years |
|---|---|---|---|---|---|---|---|---|
| **Tephra K1a** | | | | | | | | |
| SUERC 14084 | b | 15-4P | 368-369 | Gb | 7906 ± 36 | 8419 (e) | | |
| **Tephra K1b** | | | | | | | | |
| SUERC 11335 | a | 12-1K | 216-217 | Gb | 7959 ± 35 | 8463 (e) | | |
| **Tephra not analysed** | | | | | | | | |
| SUERC 14101 | c | 17-5P | 750-751 | Gb | 8823 ± 39 | 9538 (e) | | |
| **Saksunarvatn ash** | | | | | | | | |
| SUERC 14104 | d | 17-5P | 862-863 | Gb | 9728 ± 39 | 10297 ± 118 | 9194 ± 16 | 534 ± 124 |
| SUERC 21416 | d | 15-4P | 426-427 | Gb | 9739 ± 38 | 10297 ± 118 | 9206 ± 16 | 533 ± 124 |
| SUERC 11342 | a | 12-1K | 480-481 | Gb | 9752 ± 35 | 10447 ± 118 | 9277 ± 16 | 475 ± 123 |
| **Vedde ash** | | | | | | | | |
| SUERC 14087 | b | 15-4P | 458-459 | Nps | 10965 ± 40 | 11934 ± 125 | 10166 ± 24 | 799 ± 131 |
| SUERC 21419 | d | 15-4P | 463-464 | Nps | 11808 ± 41 | 12208 ± 168 | 10372 ± 22 | 1436 ± 173 |
| SUERC 21430 | d | 10-1P | 98-99 | Nps | 11566 ± 40 | 12120 ± 90 | 10343 ± 31 | 1223 ± 99 |
| SUERC 14108 | d | 17-5P | 954-955 | Nps | 11897 ± 42 | 12317 ± 309 | 10393 ± 18 | 1504 ± 312 |
| **Tephra K2** | | | | | | | | |
| SUERC 21432 | d | 10-1P | 128-129 | Nps | 12583 ± 41 | 12600 ± 125 | 10678 ± 78 | 1905 ± 132 |
| **Onset Younger Dryas** | | | | | | | | |
| SUERC 14089 | a | 15-4P | 472-473 | Gb | 11811 ± 42 | 12833 ± 125 | 10970 ± 66 | 841 ± 132 |
| **Tephra R1** | | | | | | | | |
| SUERC 21421 | d | 15-4P | 485-486 | Nps | 11793 ± 49 | 13614 ± 126 | 11746 ± 56 | 47 ± 135 |
| **Tephra K3** | | | | | | | | |
| SUERC 14090 | a | 15-4P | 500-501 | Nps | 12636 ± 43 | 14000 ± 127 | 12150 ± 55 | 486 ± 138 |
| **(Bølling warm interval)** | | | | | | | | |
| SUERC 21427 | d | 15-4P | 507-508 | Nps | 12487 ± 43 | 14263 ± 127 | 12418 ± 58 | 69 ± 138 |
| **Mid - Tephra G2/3** | | | | | | | | |
| SUERC 14098 | d | 10-1P | 192-193 | Nps | 13479 ± 47 | 14690 ± 127 | 12508 ± 69 | 971 ± 139 |
| SUERC 21428 | d | 15-4P | 515-516 | Nps | 14281 ± 44 | 14822 ± 262 | 12502 ± 91 | 1779 ± 266 |
| SUERC 14110 | d | 17-5P | 978-979 | Nps | 13528 ± 45 | 14928 ± 262 | 12560 ± 99 | 968 ± 266 |
| **Pre - Tephra G3** (518 cm in 15-4P) | | | | | | | | |
| SUERC 14091 | b | 15-4P | 520-521 | Nps | 14657 ± 48 | 15253 ± 311 | 12574 ± 100 | 2083 ± 315 |
| **St.2-23.5 (27.3 ka)** | | | | | | | | |
| SUERC 14117 | d | 17-5P | 1103-1104 | Nps | 23860 ± 107 | 27310 ± 579 | 22542 ± 126 | 1318 ± 588 |

606 (a) Thornalley et al., 2009; (b) Thornalley et al., 2010a; (c) Thornalley et al., 2010b; (d)
607 this study; (e) no independent stratigraphic age control therefore age models were based
608 on the $^{14}C$ dates assuming a 400 year surface ocean reservoir age. Nps,
609 *Neogloboquadrina pachyderma* sinistral; Gb, *Globigerina bulloides*.
610

611 **Fig.1.**

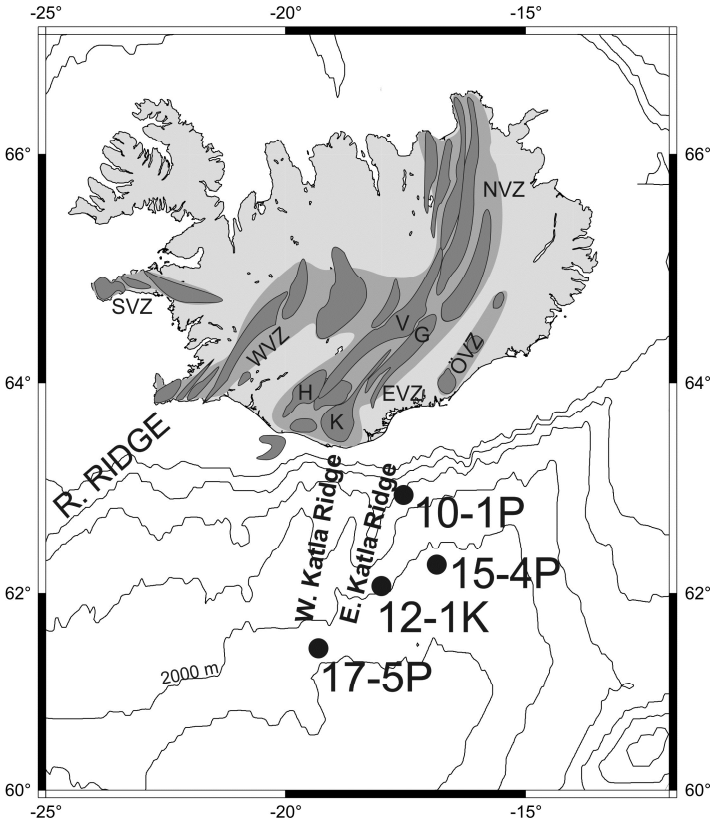


612

613 **Fig. 1.** Study area and core locations (RAPiD prefixes have been removed from core
614 names; 400 m bathymetric contours shown). EVZ, Eastern Volcanic Zone; NVZ,
615 Northern Volcanic Zone; WVZ, Western Volcanic Zone; SVZ, Snæfellsnes Volcanic
616 Zone; and ÖVZ Öræfajökull-Snæfell Volcanic Zone. The major volcanic systems are
617 shown in dark grey: G, Grímsvötn; H, Hekla; K, Katla; and V, Veidivötn. After Larsen
618 and Eiríksson (2009), modified from Jóhannesson and Sæmundsson (1998).

**Fig. 2.**

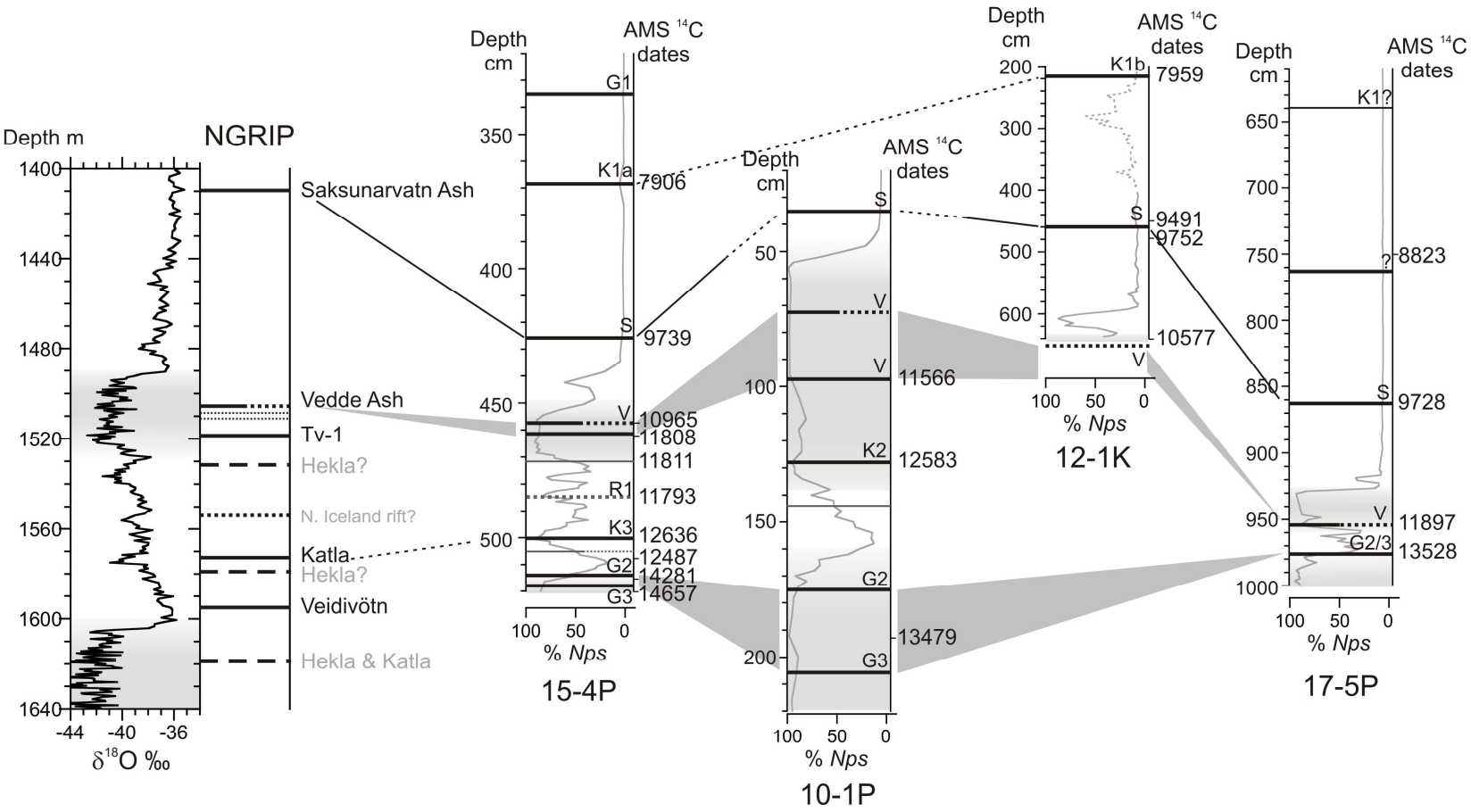


**Fig. 2.** Tephra stratigraphy for the South Iceland Rise RAPiD cores and NGRIP ice core (Mortensen et al., 2005) and the likely volcanic sources. Percent abundance of *N. pachyderma* (sinistral) shown in grey was correlated to changes in NGRIP $\delta^{18}O$; light grey shading indicates the YD and Heinrich Stadial 1 cold intervals. Tephra layers identified visually or by grain counts: solid lines, basaltic tephra; dashed lines, intermediate tephra; dotted lines, rhyolitic tephra. Thin lines indicate possible tephra layers where small increases in tephra abundance were detected. Tephra layer labels: G, Grímsvötn tephra; K, Katla tephra; R, rhyolite; S, Saksunarvatn ash; V, Vedde ash. $^{14}C$ are not calibrated to calendar years or corrected for surface ocean reservoir effects. RAPiD suffixes have been removed from core names.

627 **Fig. 3.**

628

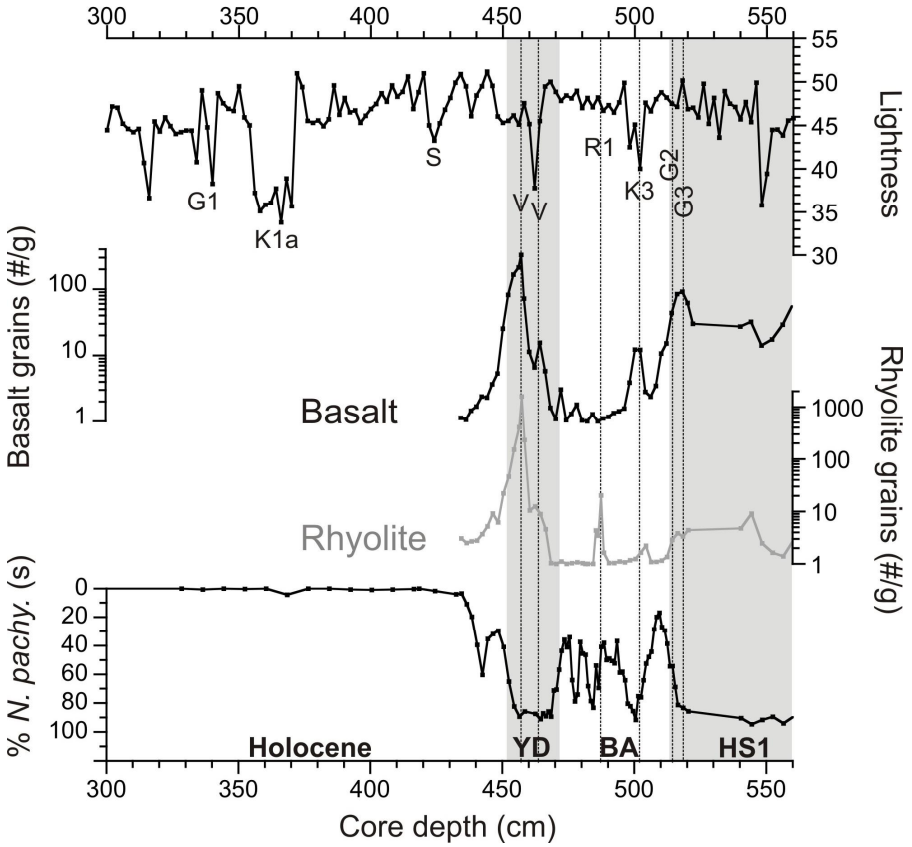


629

630 **Fig. 3.** Tephra grain counts (150-250 μm size fraction) per gram of dry sediment and colour
631 reflectance data (lightness) for RAPiD-15-4P. Tephra layer labels: G, Grímsvötn tephra; K,
632 Katla tephra; R, rhyolite; S, Saksunarvatn ash; V, Vedde ash. YD, Younger Drays; BA,
633 Bølling-Allerød; HS1, Heinrich Stadial 1.

634

635 **Fig. 4.**

636

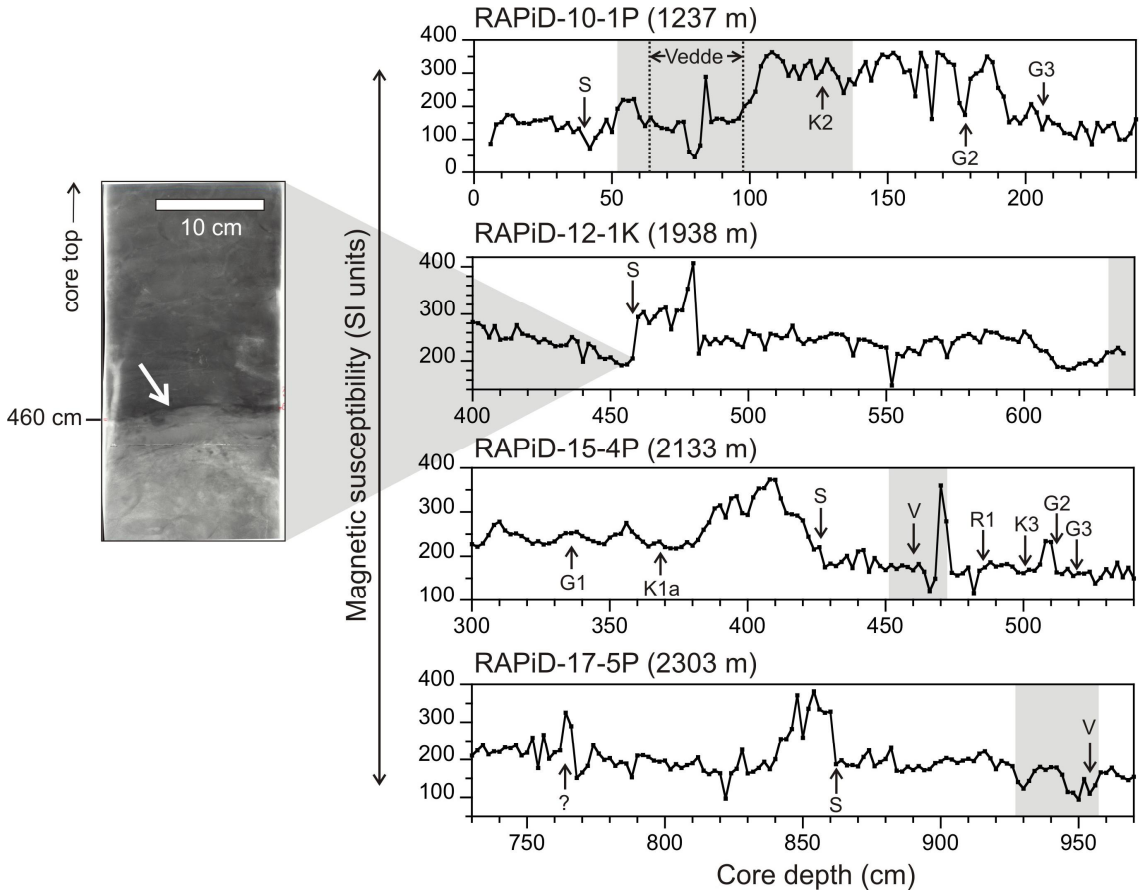


637

638 **Fig. 4.** Magnetic susceptibility for the South Iceland Rise RAPiD cores. The Younger Dryas
639 cold interval is indicated by grey shading. Tephra layer labels: G, Grímsvötn tephra; K, Katla
640 tephra; R, rhyolite; S, Saksunarvatn ash; V, Vedde ash. Also shown is an X-radiograph
641 showing the onset of the Saksunarvatn ash in RAPiD-12-1K. (The increase in magnetic
642 susceptibility in RAPiD-12-1K at 480 cm is caused by an abrupt increase in flow speed, and
643 the later onset of the Saksunarvatn ash at 460 cm is associated with a decrease in magnetic
644 susceptibility.)

645

646 **Fig. 5.**

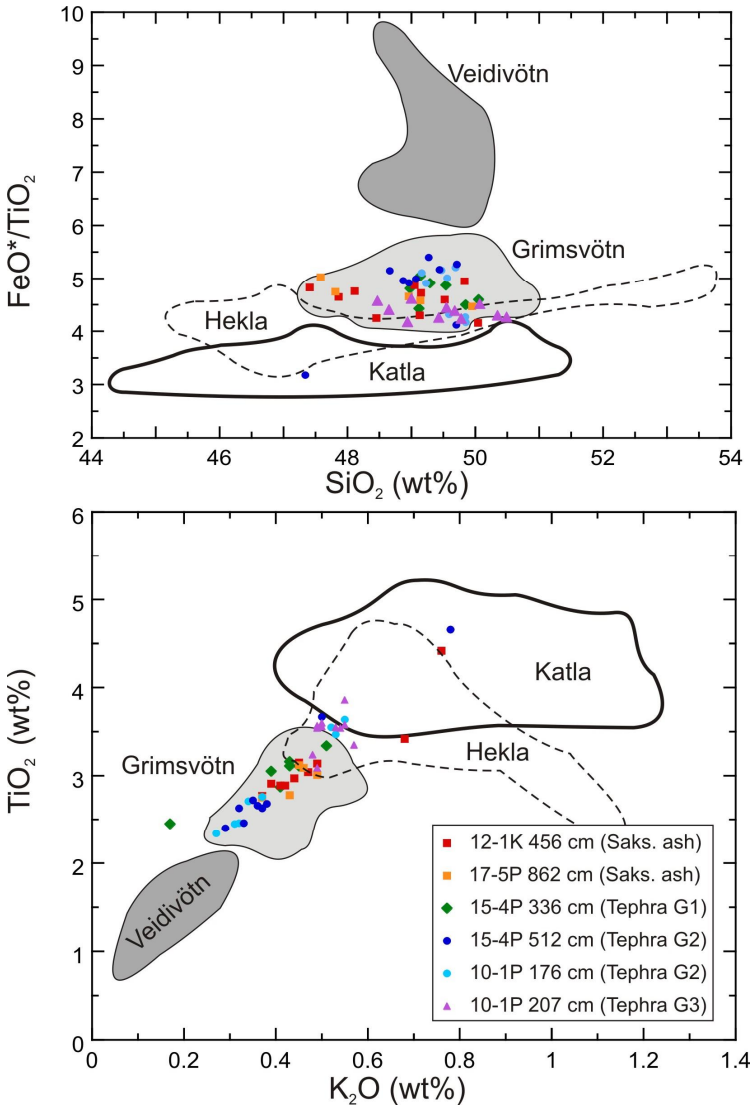


647

648 **Fig. 5.** Geochemical data for the basaltic tephra layers primarily sourced from Grímsvötn.
649 FeO*, total iron. Geochemical envelopes for the source volcanoes are taken from Davies et
650 al. (2010) and reference therein.

651

**Fig. 6.**

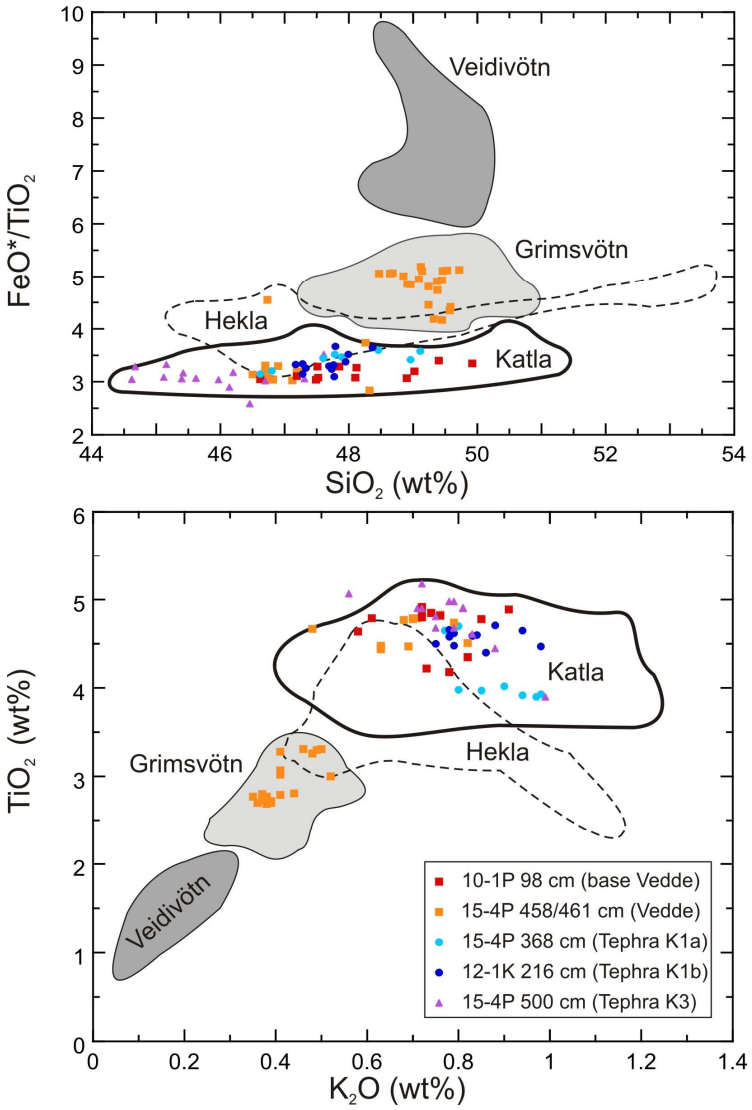


**Fig. 6.** Geochemical data for the basaltic tephra layers primarily sourced from Katla. FeO*, total iron. The mixed Katla-Grímsvötn signal for 15-4P 458/461 cm (Vedde ash) is caused by a basaltic turbidite. Geochemical envelopes for the source volcanoes are taken from Davies et al. (2010) and reference therein.

**Fig. 7.**

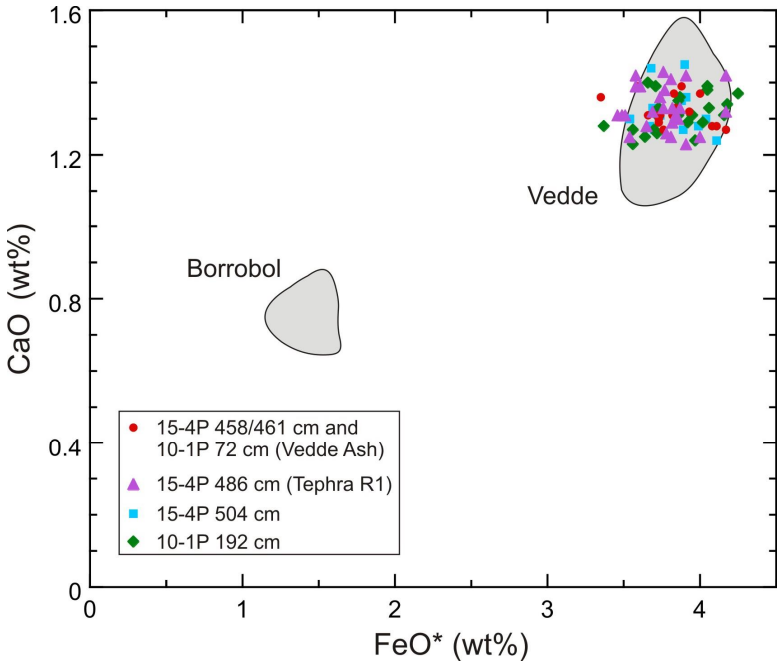


**Fig. 7.** Geochemical data for the rhyolitic tephra deposited in the deglacial sections of the South Iceland Rise RAPiD cores. FeO*, total iron. Geochemical envelopes for the source volcanoes are taken from Koren et al. (2008) and reference therein.

**Fig. 8.**

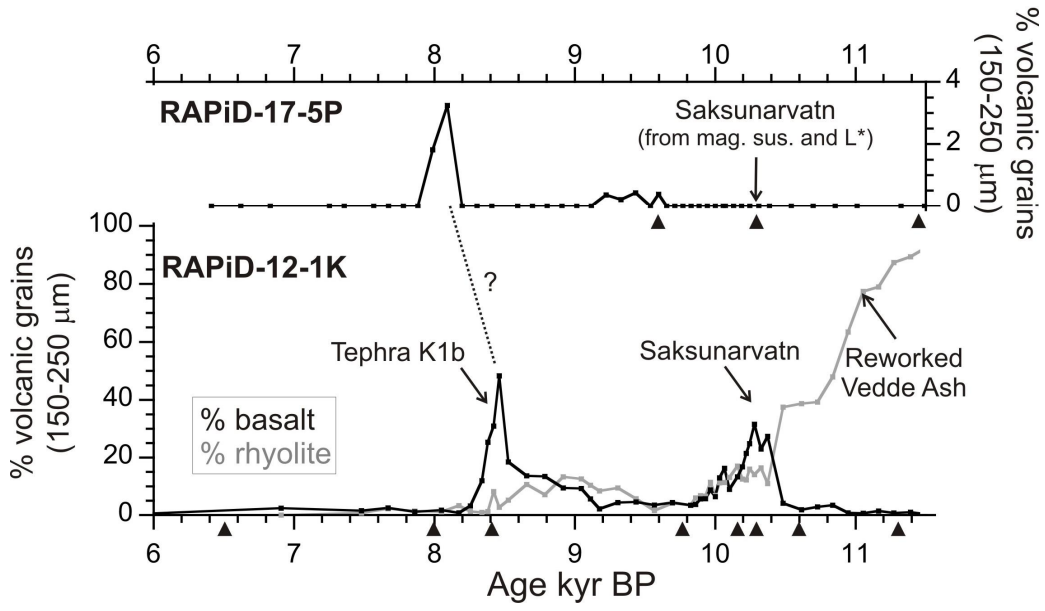


**Fig. 8.** Possible correlation of tephra K1b found in core 12-1K with an increase in basalt grains in core 17-5P at ~8 ka. Age control points for the cores are indicated by the black triangles. Core 17-5P also has a planktonic foraminifera $^{14}C$ date at 3.57 ka (not shown) so the age of the peak at 8.1 ka is very approximate, being based on a linear sedimentation rate from 9.54 to 3.57 ka.

673 **Fig. 9.**

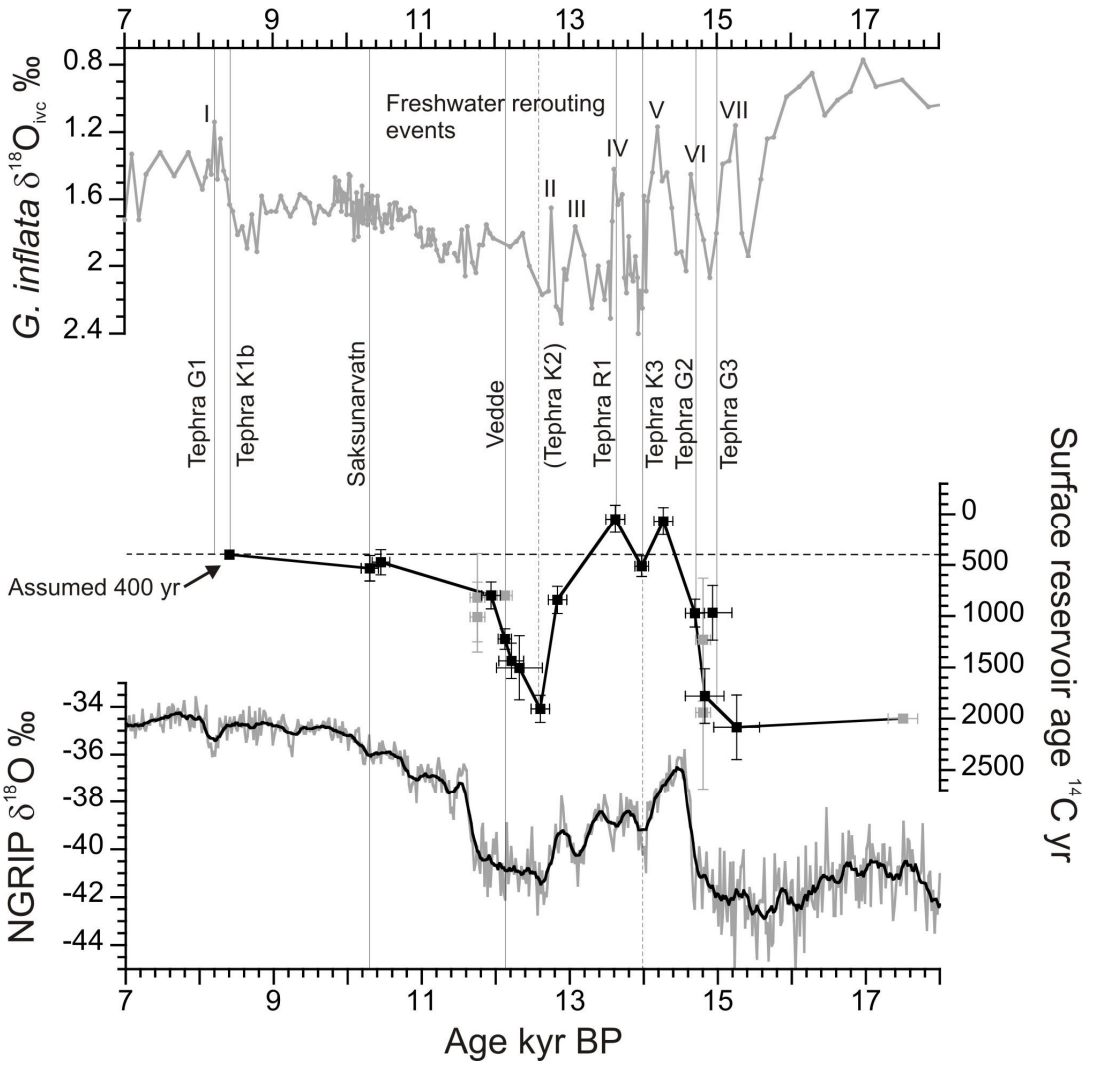


674

675 **Fig. 9.** Deglacial surface ocean radiocarbon reservoir ages ($R_{surf}$) for the South Iceland Rise.
676 Dashed horizontal line indicates modern $R_{surf}$ south of Iceland of ~400 years. Error bars
677 include $^{14}C$ measurement error; errors in IntCal ô09; uncertainty in the independent age model
678 tie to NGRIP, accounting for the abruptness of the transition, sedimentation rates and
679 estimated biotubation effects; and errors in annual layer counting of NGRIP, using the
680 assumption that counting errors are not correlated between different climate intervals
681 (Rasmussen et al., 2006). $R_{surf}$ values from Bard et al. (1994) and Waelbroeck et al. (2001)
682 are shown in grey. Tephra layers are indicated by vertical black lines. The *Globorotalia*
683 *inflata* ó ice-volume corrected ô $\delta^{18}O$ record from Thornalley et al. (2010a) is also presented at
684 the top of the figure to show the relative timing of the tephra layers in the RAPiD cores with
685 respect to the reconstructed freshwater rerouting events (numbered).